



Since January 2020 Elsevier has created a COVID-19 resource centre with free information in English and Mandarin on the novel coronavirus COVID-19. The COVID-19 resource centre is hosted on Elsevier Connect, the company's public news and information website.

Elsevier hereby grants permission to make all its COVID-19-related research that is available on the COVID-19 resource centre - including this research content - immediately available in PubMed Central and other publicly funded repositories, such as the WHO COVID database with rights for unrestricted research re-use and analyses in any form or by any means with acknowledgement of the original source. These permissions are granted for free by Elsevier for as long as the COVID-19 resource centre remains active.



Evolution of infectious bronchitis virus in Taiwan: Characterisation of RNA recombination in the *nucleocapsid* gene

Shu-Ming Kuo^a, Ching-Ho Wang^b, Ming-Hon Hou^c, Yuan-Pin Huang^b,
Hsiao-Wei Kao^{a,*}, Hong-Lin Su^{a,*}

^a Department of Life Sciences, National Chung Hsing University, 250 Kuo Kuang Rd., Taichung 40227, Taiwan

^b School of Veterinary Medicine, National Taiwan University, Taipei, Taiwan

^c Institute of Genomics and Bioinformatics, National Chung Hsing University, Taichung, Taiwan

ARTICLE INFO

Article history:

Received 13 June 2009

Received in revised form 5 February 2010

Accepted 16 February 2010

Keywords:

Infectious bronchitis virus

RNA recombination

Coronavirus

Nucleocapsid

ABSTRACT

Avian infectious bronchitis virus (IBV) belongs to the *Coronaviridae* family and causes significant economic loss in Taiwan (TW), even in flocks that have been extensively immunised with Massachusetts (Mass)-serotype vaccines. Phylogenetic analysis of all non-structural and most structural genes shows that TW IBV is genetically distinct from the US strain and more similar to Chinese (CH) IBV. In contrast, the *nucleocapsid* (*N*) gene of TW IBV presents phylogenetic incongruence. RNA recombination at the 5' end of the *N* gene between TW and US IBV is shown to be responsible for this discordance. Surprisingly, the recombinant *N* gene is found in all of tested TW IBV isolates, suggesting that a recombination event gave origin to a founder lineage. Our data indicate that RNA recombination in the recombinant 5' end of the *N* gene may have caused the emergence of the current IBV population in Taiwan.

© 2010 Elsevier B.V. All rights reserved.

1. Introduction

Infectious bronchitis virus (IBV) is highly contagious and pathogenic in chickens. Although the current Massachusetts (Mass)- and Connecticut-serotype vaccines usually offer sufficient protection, they are less effective in certain areas, such as China (CH) and Taiwan (TW) (Wang et al., 1996; Wang and Khan, 2000; Yu et al., 2001). Frequent point mutations and evolutionary fitness in the hypervariable regions (HVRs) of the *spike 1* (*S1*) gene contribute to most of the antigenic determinants of IBV. Therefore, the *S1* gene is often referred to as the index of genetic diversity and of viral evolution, due to its high variability and close genotype/serotype correlation (Dolz

et al., 2008; Liu et al., 2006; Wang and Huang, 2000; Wang and Tsai, 1996).

In addition to point mutation, RNA recombination is also involved in the generation of new antigenic variants. RNA recombination in a coronavirus was first demonstrated experimentally in mouse hepatitis virus (MHV) (Lai et al., 1985; Makino et al., 1986), and a high frequency of recombination was found both *in vitro* and *in vivo* after MHV infection (Keck et al., 1988; Makino et al., 1986). Recombination sites were detected throughout nearly the entire genome, and many recombinants with multiple crossover sites were found (Liao and Lai, 1992). The high frequency of RNA recombination in coronaviruses is likely caused by the unique mechanism of RNA synthesis, which involves discontinuous transcription and polymerase jumping (Cavanagh, 2007; Lai et al., 1985; Liao and Lai, 1992; Makino et al., 1986). Putative IBV genetic recombination in the *S* gene has been documented in different field isolates, including a Japanese strain (KB8523), European

* Corresponding authors. Tel.: +886 4 22840416; fax: +886 4 22854391.
E-mail addresses: hkao@dragon.nchu.edu.tw (H.-W. Kao),
suhonglin@nchu.edu.tw (H.-L. Su).

isolates (Dutch D207 and British 6/82), Texas local strains (PP14 and SE17) and a New York isolate (CU-T2) (Jia et al., 1995; Kusters et al., 1990; Wang et al., 1993), based on sequence comparison and phylogenetic incongruence. Additionally, half of the *nucleocapsid* (*N*) gene of CU-T2 was further shown to be replaced by that of the Holland 52 (H52) vaccine strain, indicating that genomic RNA recombination in IBV may occur in multiple genes (Jia et al., 1995). In Taiwan, phylogenetic analysis revealed that few TW IBV strains, such as 2992/02 and 3374/05, may undergo genetic recombination with CH IBV (Chen et al., 2009; Huang et al., 2004). This experimental evidence and the sporadic detection of recombinant variants in nature support the notion that recombination occurs in coronaviruses (Kottier et al., 1995). However, available evidence remains insufficient to allow the conclusion that coronavirus evolution can be driven by interspecies recombination.

TW IBV, first isolated in 1964 (Lu et al., 1993), can be classified into two individual serological groups, TW I and TW II, based on the sequences of the HVRs of the S1 proteins (Wang and Huang, 2000). The Mass-serotype vaccine has shown a modest protective effect on the IBV outbreak in Taiwan (Huang and Wang, 2006; Lin et al., 2005), possibly due to the considerable variation in S1 sequences between TW and US strains. In this study, we analyse TW IBVs and show that they are genetically closer to CH isolates than to US strains. The *N* gene of TW IBV is the only exception and shows phylogenetic incongruence. We further demonstrate that RNA recombination has contributed to this genetic discordance. The recombinant *N* gene is detected in all the analysed TW IBVs, suggesting that RNA recombination drives the evolution of this coronavirus at the population level.

2. Materials and methods

2.1. IBV strains

TW IBV strains were isolated and propagated through the allantoic sac route by inoculating 9–11-day-old specific pathogens free (SPF) embryonated eggs from the Animal Health Research Institute, Council of Agriculture in Taiwan (Gelb and Jackwood, 1998). TW IBVs had been purified by three consecutive limiting dilutions (Wang and Huang, 2000; Wang and Tsai, 1996). Sequences of both US and CH IBVs were obtained from Genbank maintained by NCBI.

We listed the tested IBVs and their Genbank numbers in supplementary Table 1, including 29 TW strains, 15 US strains and 30 CH strains. Inquired from the Genbank up to 2009, we found 12 TW and 15 US IBVs are decoded in both S1 and *N* genes and we included all these up-to-date IBVs in this study. Among the 12 TW strains, 8 IBVs in the same clade of ME tree (supplementary Fig. S1) were chosen for the analysis of *N* gene in Figs. 3 and 4. Both TW2992/02 and TW3374/05 were excluded because of their phylogenetic discordance in S1 (Fig. S1). Both 2994/02 and 3382/06 was excluded due to the discordance in *N* (Fig. S2). The length of the tested genes is all intact and no 3'-UTR deletion was found in these IBV strains.

2.2. Sequencing of TW2575/98

Total RNA was extracted from TW2575/98-infected allantoic fluid using TRIzol™ C&T (Protech, Taiwan), according to the manufacturer's protocol. RNA (0.5 µg) was reverse transcribed into cDNA using SuperScript™ III reverse transcriptase (RT) (Invitrogen, USA). PCR was performed with a proofreading DNA polymerase (KOD-Plus, Toyobo, Japan). Generally, the PCR conditions included 28 cycles of 94 °C for 30 s, 62 °C for 30 s, and 68 °C for 1 min, on a PCR machine (ASTEC 818, Japan). Consecutive viral genomic fragments were cloned into the pCRII-TOPO vector (Invitrogen, USA) by TA cloning and were subjected to sequencing.

The 5'-untranslated regions (UTR) of IBV 2575/98 was analysed using a SMART™ RACE cDNA amplification kit (Clontech, USA). First, cDNA was prepared from 1 µg of total RNA from allantoic fluid, using the PowerScript™ RT and a unique 3' reverse primer (5'-TAC TTG CAA GAC AAG TTC C-3', nt 1247–1265 of the viral genome). After the RT reached the 5' end of the mRNA template, it added 3–5 dC residues to the newly synthesised cDNA. The SMART II A 5' oligonucleotide (5'-AAGCAGTGGTATCAACGCAGAGTACGCGGG-3') annealed to the dC tag and served as an additional extending primer for RT. Consequently, the 5' single-stranded cDNA was used as the PCR template with the nested primer (5'-AAGCAGTGGTATCAACGCAGAGT-3') and a new reverse primer, 5'-CCAACAAGCTGCGCATTGCCATAG-3' (nt 996–1020 of the viral genome). Amplified DNA products were cloned into the pGEM-T Easy Vector (Promega, USA) and sequenced.

2.3. Phylogenetic analysis

Phylogenetic trees were constructed by Bayesian inference (BI), maximum likelihood (ML) and minimum evolution (ME) methods. The best-fit models and parameters for initial settings of the phylogenetic programs were selected by Modeltest 3.7 for BI and ML algorithms on the basis of the Akaike information criterion (Posada and Crandall, 1998).

Estimates of evolutionary divergence over all sequence pairs were computed by averaging the number of base substitutions per site in MEGA 4.0. All positions containing gaps and missing data were eliminated from the dataset. Standard error estimates were obtained by a bootstrap procedure from 500 replicates.

For the S1 data set in Fig. 1A, the best-fit model of substitution was a GTR model (Rodriguez et al., 1990) with a gamma substitution parameter (α) of 1.2894, a proportion of invariable sites (*I*) of 0.3152, and base frequencies of A: 0.2856, C: 0.175, G: 0.1862 and T: 0.3532. For the full-length *N* data set, the best-fit model was a GTR model with $\alpha = 0.6953$, *I* = 0.3808, and base frequencies of A: 0.3135, C: 0.1937, G: 0.2537 and T: 0.2391. For nt 1–600 of *N*, the best-fit model was a TIM model (Rodriguez et al., 1990) with $\alpha = 0.5349$, *I* = 0.3677, and base frequencies of A: 0.3100, C: 0.1953, G: 0.2460 and T: 0.2488. For nt 601–1230 of *N*, the best-fit model was a GTR model with $\alpha = 0.3746$, *I* = 0.8688, and base

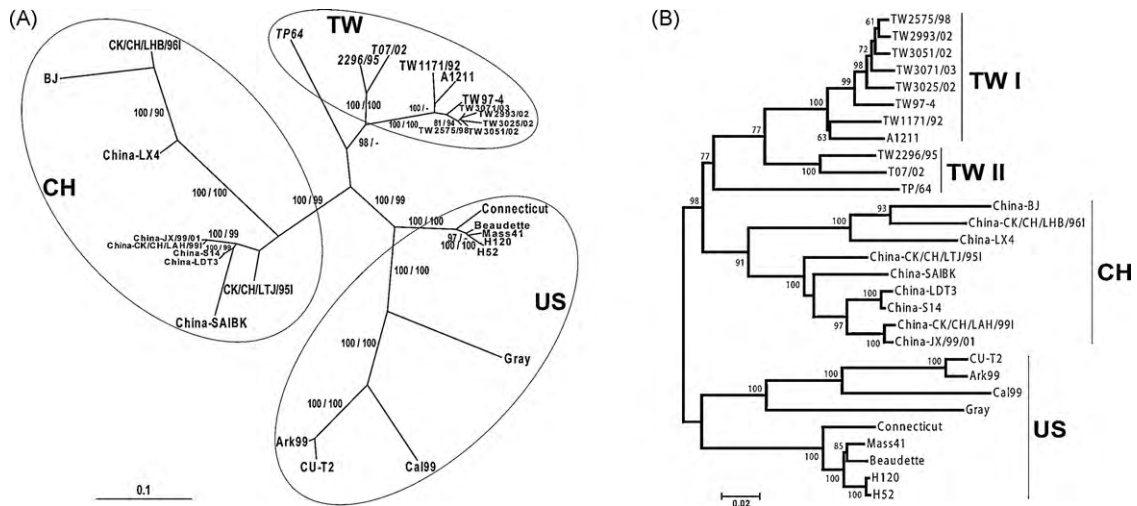


Fig. 1. Phylogenetic relationships among the *S1* genes of IBVs. (A) The phylogenetic tree, based on Bayesian inference, shows relationships among the three major groups, Taiwanese (TW I and II), Chinese (CH) and American (US). Supporting values are shown in the form of Bayesian posterior probability/maximum likelihood bootstrap. (B) Bootstrap values, estimated from 1000 replicates of the ME analysis in MEGA 4.0, are given (only values >60 are shown). The scale bar indicates the number of nucleotide replacements per site.

frequencies of A: 0.3230, C: 0.1849, G: 0.2594 and T: 0.2327.

MrBayes 3.1.2 was used for BI analysis. Random starting trees were used. A total of two million generations of Markov chains were run. Trees were saved every 100 generations, resulting in 20,000 trees in the initial samples. The stationary phase of log-likelihood was reached within 500,000 generations. Thus the burn-in (number of initial trees that were discarded) was set to 5000. A majority-rule consensus tree was generated from the remaining samples (15,000 trees), and the percentage of samples recovering any particular clade represented the clade's posterior probability.

We conducted 500 nonparametric bootstrap replicates for ML analysis using GARLI v0.951. We used the heuristic search option with substitution models set to the best-fit model chosen by Modeltest 3.7. ME analysis was performed using MEGA 4.0 with 500 replicates.

2.4. Recombination detection

Twelve IBV strains, including TW2575/98, TW1171/92, TW2296/95, TP/64, Mass 41, Cal99, Beaudette, CU-T2, CH-BJ, CH-S14, CH-LX4 and CH-LDT3, were subjected to the Recombination Detection Program (RDP) 3.0 (Martin and Rybicki, 2000). Genes *S* and *N* were aligned by ClustalW and analysed by seven algorithms in RDP 3.0, including RDP, Bootscan, GENECONV, MaxChi, Chimaera, SiScan, and 3Seq. Based on the results automatically calculated by RDP, TW2575/98, TW2296/95, CU-T2 and CH-LX4 were chosen as representative strains for which data is shown below. Data were further subjected to the Genetic Algorithms for Recombination Detection (GARD) program to confirm the putative single breakpoint position (Kosakovsky Pond et al., 2006).

3. Results

3.1. Phylogenetic analysis of *S1* genes

To elucidate the phylogenetic relationships of TW IBV, 74 IBVs were analysed in this study, including 29 TW strains, 30 CH strains and 15 US strains. Minimum evolution (ME) test showed that 25 TW IBVs form a unique branch independent of the US and CH groups (Fig. S1). Some exceptional strains showing the phylogenetic incongruence were noticed, such as the TW2992/02 (Chen et al., 2009; Huang et al., 2004), TW2994/02 (Huang et al., 2004), TW3374/05 (Chen et al., 2009), China CK/CH/LDL971 and China CK/CH/LDL981 (Chen et al., 2009). In their respective clades, 11 TW strains, 9 CH strains, 9 US strains were chosen for the analyses of nucleotide-sequence identity, maximum likelihood (ML) and Bayesian inference (BI). The nucleotide-sequence identity between TW *S1* genes and those of US or CH isolates was similar (77–82%). The phylogenetic tree shown in Fig. 1A, which were constructed by BI, shows that TW IBV is a branch independent of the US and CH groups. Analysis of ML reproduces similar tree topology and the bootstrap values are illustrated together with the posterior probability (Fig. 1A). Interestingly, the evolutionary divergence and ME methods indicated that TW IBVs are more closely related to the CH cluster than to the US group (Table 1, Fig. 1B and Fig. S1), supported by less difference between TW-CH strains (Table 1) and the high bootstrap value (98%) for the branch separating the TW-CH groups from US group (Fig. 1B), respectively.

3.2. Non-structural genes *1a* and *1b* and structural genes *E* and *M*

A virulent Taiwanese field isolate, TW2575/98, was fully sequenced (27,710 bps; DQ646405). The G/C content

Table 1The evolutionary divergence of the *SI* and *N* genes between IBV groups.

Gene	Group		
	TW-US	TW-CH	US-CH
<i>SI</i>	0.194 ± 0.007	0.179 ± 0.007	0.203 ± 0.007
<i>N</i> 1–1230 nt	0.110 ± 0.007	0.131 ± 0.007	0.124 ± 0.007
<i>N</i> 1–600 nt	0.080 ± 0.008	0.128 ± 0.011	0.121 ± 0.011
<i>N</i> 601–1230 nt	0.138 ± 0.011	0.135 ± 0.011	0.127 ± 0.010

of the viral genome was 38.5%. ORFs *1a*, *1b*, *E* and *M* of TW2575/98 were compared to those of other IBV genomes (Fig. 2). Phylogenetic trees of the *1a* and *1b* genes of TW IBVs consistently show a closer relationship to the CH strains than to the US strains (Fig. 2A and B). Analysis of the 5'-UTR and the ORF 1-encoded proteins (including the papain-like proteinase, helicase, RNA-dependent RNA polymerase, p58 and HD2 protein) using the neighbour-joining algorithm reproduces the same topology (data not shown). Similar results are also seen in the trees based on the full-length *E* and *M* genes of IBV, as shown in Fig. 2C and D, further illustrating that TW IBV is genetically closer to the CH virus.

3.3. Phylogenetic analysis of *N*

In contrast to the above results, the *N* gene of TW IBV showed surprising phylogenetic incongruence and was more closely related to that of US isolates according to the ME algorithm (Fig. S2, Fig. 3A and B) and the evolutionary divergence analysis (Table 1). A fragment containing nt 1–600 and its encoded proteins (Fig. 3C and D) also reflected

the same phylogenetic relationship as the full-length *N* region. Interestingly, results based on the 3'-terminus of the TW IBV *N* gene and its encoded protein (Fig. 3E and F) were inconsistent with those from the full-length *N* gene, and were similar to those for the genes described above and shown in Figs. 1 and 2.

To further examine this phenomenon, unrooted phylogenetic trees produced by BI clearly illustrate that the TW *N* gene is phylogenetically closer to US IBV than to CH IBV (Fig. 4A, C and E). Crucially, Fig. 4C illustrates that the 5'-termini of the *N* genes of TW and US IBV belong to the same monophyletic group, rather than being separate isolated branches.

The K_a/K_e ratio of TW2575/98 *N* versus all IBVs analysed in this study is 0.06–0.17, indicating the purifying selection of *N* protein during evolution. To further clarify whether the phylogenetic incongruence is caused by different evolutionary rates in different parts of the *N* gene, a ML test that are not biased by evolutionary rate variation was applied to recheck the phylogenetic relationships (Holmes and Rambaut, 2004). No major difference was observed between the results from the BI and those from the ML test (Fig. 4B, D and F), confirming that RNA recombination probably occurred between TW and US IBVs in the 5'-terminal region of the *N* gene and that the phylogenetic incongruence was not caused by point mutation or variation in local evolutionary rates.

3.4. Recombination in the *N* gene in TW IBVs

To further test our hypothesis, genes 5 and *N* of 12 IBVs were subjected to the Recombination Detection Program

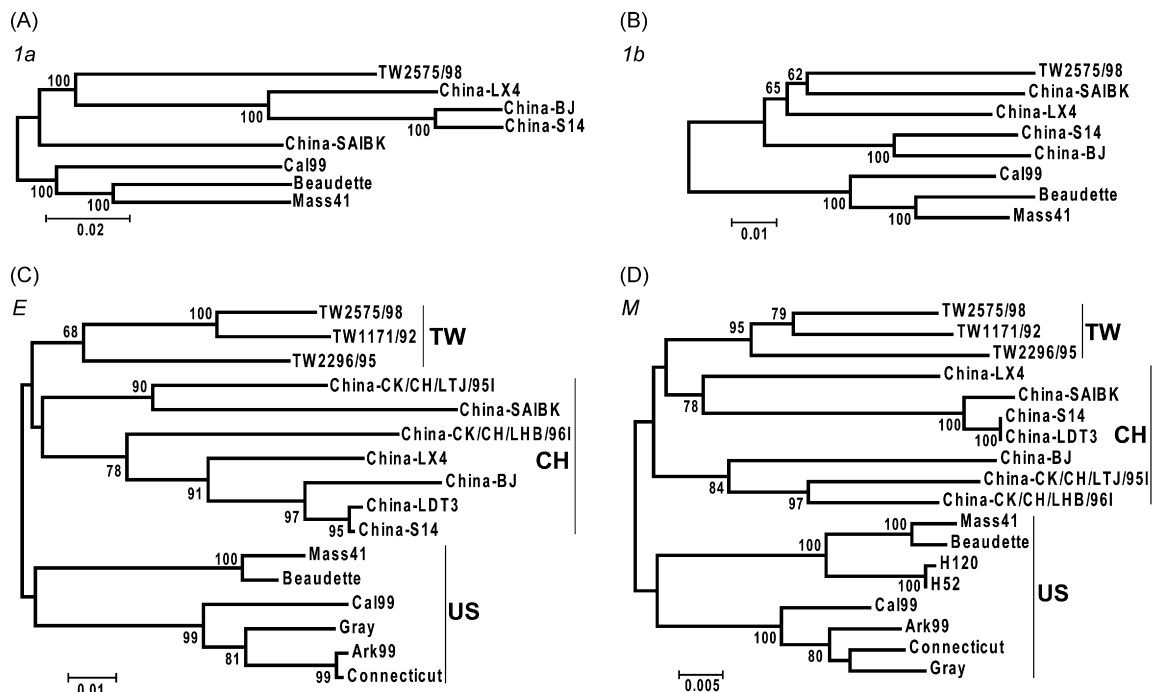


Fig. 2. Phylogenetic trees of genes *1a*, *E*, and *M* of IBVs. The trees were constructed using ME algorithms. Gene *1a* (A): the 5'-UTR and full-length sequence of *1a* (12,528 bp); *1b* (B): nt 18,782–20,459 (1678 bp); the full-length envelope (306 bp) and membrane (678 bp) genes: *E* (C) and *M* (D), respectively. Bootstrap values greater than 60% are shown. The scale bar indicates the number of nucleotide replacements per site.

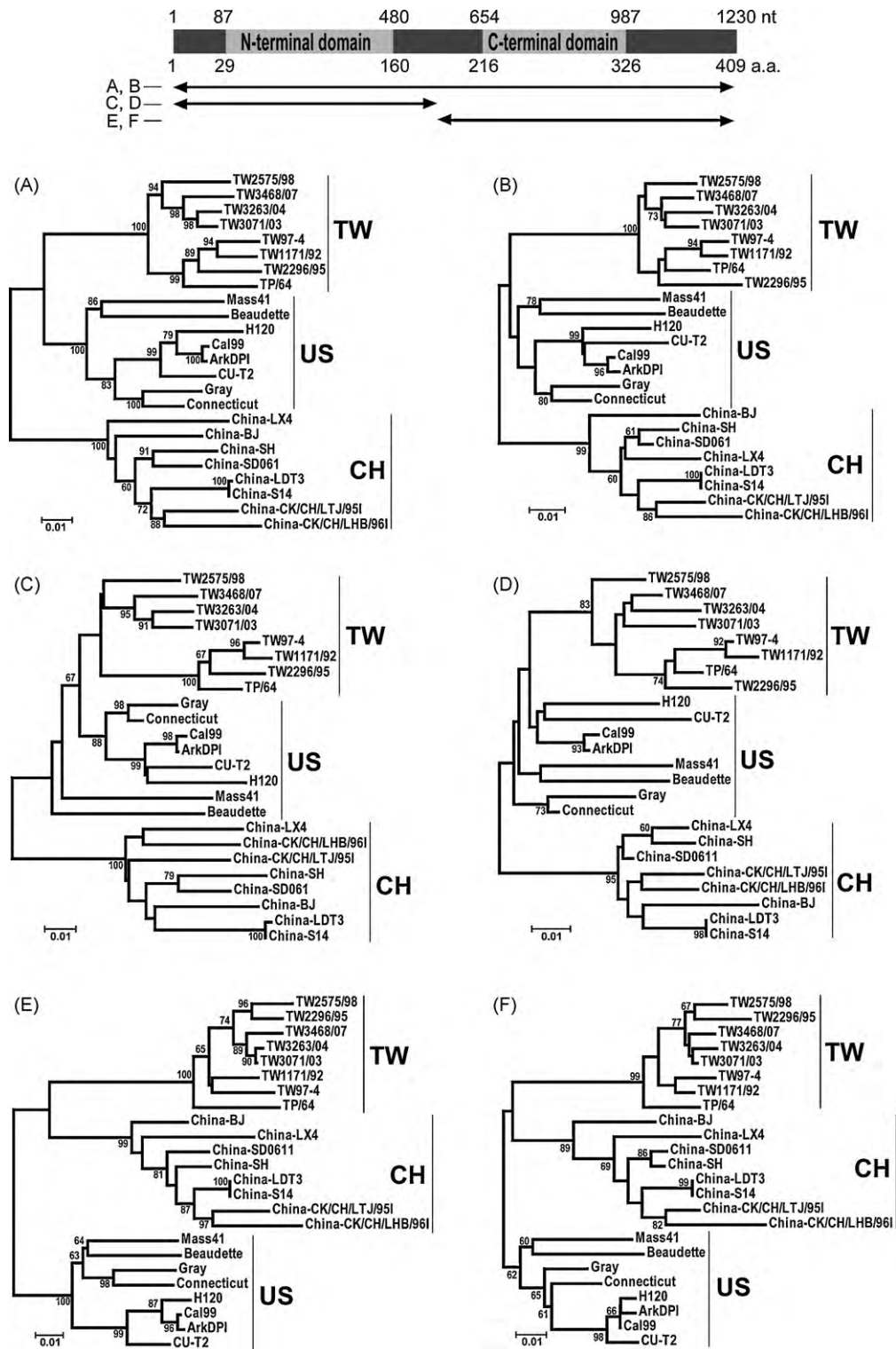


Fig. 3. ME trees of the N gene and protein of IBVs. Both genes (A, C, and E) and their encoded proteins (B, D, and F) are illustrated. full-length, nt 1–1230 (A) and aa 1–409 (B); N-terminus, nt 1–600 (C) and aa 1–200 (D); C-terminus, nt 601–1230 (E) and aa 201–409 (F). The scale bars correspond to the number of nucleotide replacements per site.

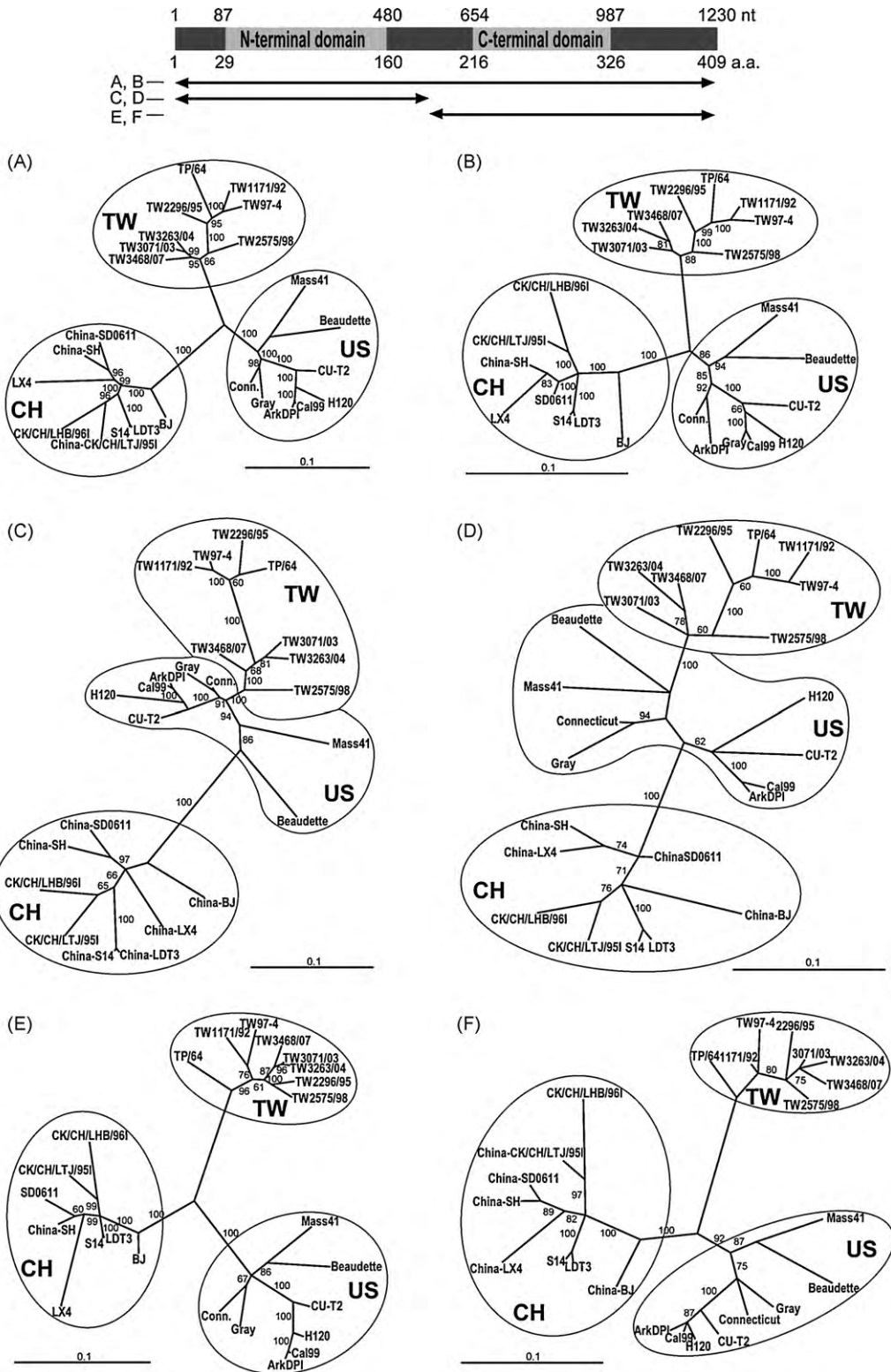
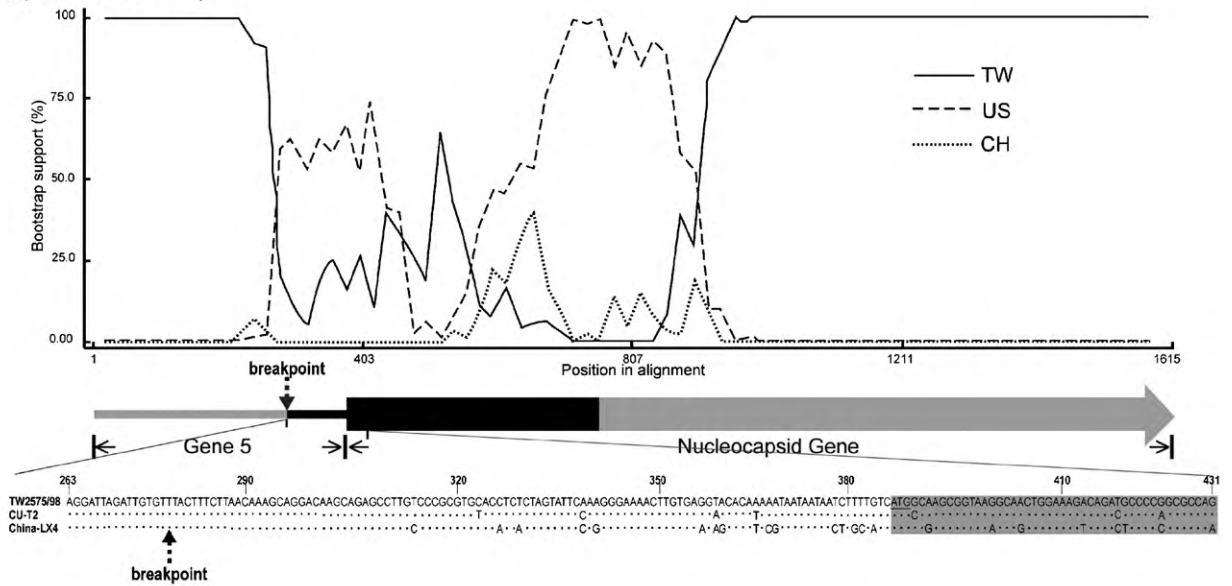
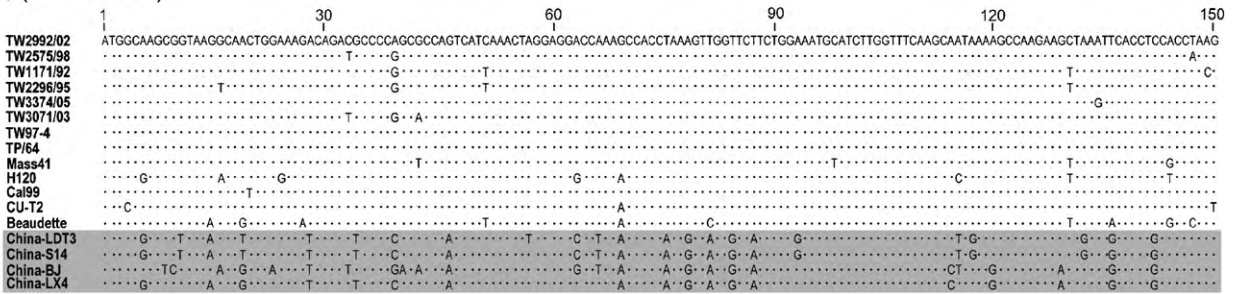


Fig. 4. Bayesian and ML unrooted trees of the N gene of IBVs. These phylogenetic reconstructions are based on BI analysis in MrBayes 3.1.2 (A, C, and E) and ML analysis in GARLI v0.951 (B, D, and F). Full-length, nt 1–1230 (A and B); N-terminus, nt 1–600 (C and D); C-terminus, nt 601–1230 (E and F). The scale bars correspond to the number of nucleotide replacements per site.

(A) (RDP/Bootscan)



(B) (N 1~150 nt)



(C) (N 1~50 aa)

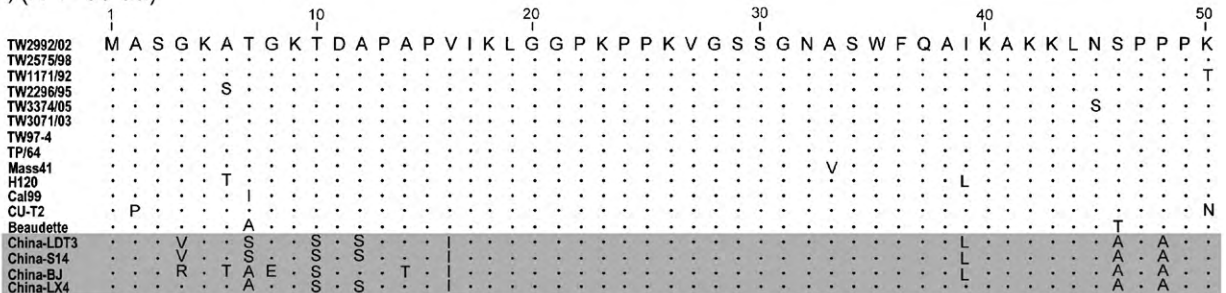


Fig. 5. Recombination and putative breakpoints within genes 5 and N of TW IBV. (A) For the RDP/Bootscan analysis, TW2575/98 was used as the query strain for potential recombination detection. TW2296/95 (solid line) and CU-T2 (dashed line) were used as parental sequences; CH-LX4 was as an outlier sequence. The black region represents a potential crossover within nt 278–757 of the queried sequences. The arrow indicates the suggested breakpoint at nt 278, proposed by both the Bootsacan and GARD programs. The N gene, starting with the underlined ATG, is shaded (A). Alignments of the first 150 nt (B) and the deduced aa sequences (C) of N are illustrated. The CH IBVs in panel B and C are shaded to highlight their discrepancy.

(RDP) (Martin and Rybicki, 2000) and the Genetic Algorithms for Recombination Detection (GARD) program (Kosakovsky Pond et al., 2006) to examine the interspecies recombination. RDP analysis and three GARD algorithms all consistently showed high significance (p value = 1.9×10^{-3} to 3.5×10^{-9}) to support the hypothesis of interspecies recombination with the breakpoint at nt 278

of gene 5. RDP-bundled algorithms also revealed one candidate crossover region between the TW and US genes, located between nt 278 and 757 of the queried sequences, covering the gene 5 and the 5'-terminus of the N gene (Fig. 5A). For instance, the p values of the RDP and Bootsacan algorithms were 5.1×10^{-4} and 1.0×10^{-5} , respectively. Alignment of the first 150 base pairs (bp) of N clearly

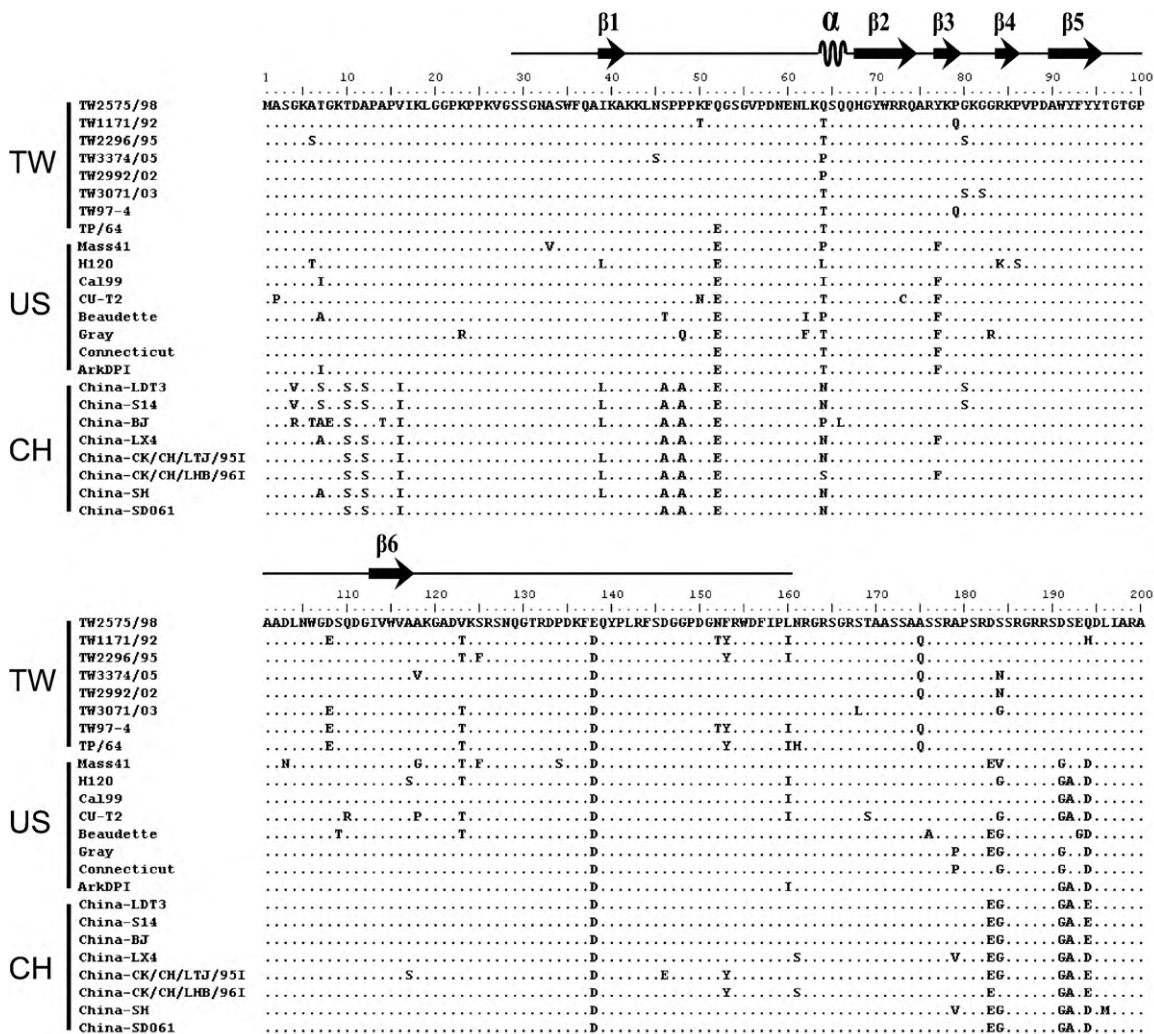


Fig. 6. Alignment of the N-termini of IBVs with N-terminal domain secondary structures. The regions of numbered β-sheets and the α-turn (α) are deduced from the N-terminal domain stereography of the Beaudette strain.

indicated high identity between the TW and US strains (Fig. 5B). Moreover, the deduced protein sequences also showed that the CH IBVs were significantly different from the TW and US strains (Fig. 5C and Fig. 6).

In addition, all the analysed TW IBVs shared the recombinant *N* gene, including one of the earliest isolates found in Taipei in 1964, TP/64 (Figs. 3 and 4). This finding suggests that the recombination in the *N* gene produced a novel IBV founder distinct from IBV lineages present before 1964. The recombination event may have provided replication benefits, enabling the offspring of this founder to become dominant.

4. Discussion

The variation in the *S1* region often represents viral genetic diversity and strain evolution (Dolz et al., 2008; Liu et al., 2006; Wang and Huang, 2000; Wang and Tsai, 1996). The ratio of K_a/K_s can be an indicator of selective pressure acting on an open reading frame. The K_a/K_s of nucleotides

in the *S1* region was $0.35 \pm 0.12\%$ among evaluated TW IBVs. Although previous studies of IBV *S1* genes have argued that TW IBV is an independent branch of the US group (Huang et al., 2004), the relationship between TW IBV and CH isolates remains unclear. In this study, we have shown that Taiwanese IBV features a recombinant NTD in the *N* locus and has evolved into a unique population. The interspecies recombination is evidenced by the incongruent phylogenetic relationship inferred for this gene region, high consensus in the N-terminus between TW and US strains, rare synonymous mutations in the conserved N protein, and well-supported results from RDP analyses.

A fast rate of mutation caused by an error-prone RNA-dependent RNA polymerase is a major factor driving the evolution of RNA viruses. Nevertheless, as the restraint of error threshold of lethal mutations, the coronavirus is speculated to have a relatively low mutation rate due to its large genome size (Eigen, 1987; Maynard Smith and Szathmáry, 1995). To increase viral adaptability and fitness, coronavirus has evolved a unique discontinuous

transcription system and 'copy-choice' genomic synthesis to achieve high efficiency of RNA recombination (Cavanagh, 2007; Lai et al., 1985; Liao and Lai, 1992; Makino et al., 1986). However, only sporadic recombinant variants have been detected in nature. We here show that the recombinant *N* gene was detected in all the isolated TW IBVs, supporting the participation of recombination in viral evolution and showing that a recombinant RNA virion can emerge as a local dominant strain.

Since the emergence of severe acute respiratory syndrome coronavirus (SARS-CoV) in humans, coronavirus has become a new focus of pathogenic research. In the present, little is known about the original strain and the natural host of the SARS-CoV. Plausibly, the SARS-CoV may have originated, like TW IBV, through RNA recombination in an unidentified host and subsequently emerged as a new virus in human beings by crossing the host boundary (Holmes and Rambaut, 2004; Hon et al., 2008; Magiorkinis et al., 2004; Stavriniades and Guttman, 2004; Zhang et al., 2005). However, present evidence is far from supporting this conclusion, and extensive sampling of the coronavirus genome from candidate hosts is required to solve this important issue.

Although studies of MHV have demonstrated that RNA recombination can occur throughout the genome, genetic crossovers in coronaviruses are usually detected after TAS sequences, referred to as putative hotspot sites (Keck et al., 1987; Kusters et al., 1990; Liao and Lai, 1992). In this study, both the RDP/BootsScan and GARD analyses suggested the possibility of a putative 5' recombination crossover nick at nt 278 of gene 5 in the TW IBV genome. Alternatively, given the remarkable discrepancy between the first 150 nt of CH *N* and those of TW and US *N* (Fig. 5), the start codon of *N* after the TAS sequence may also serve as a breakpoint candidate for genetic recombination within TW IBV genome.

It is noteworthy that one of the earliest TW IBVs, TP/64, shares high sequence identity in the first 150 nt of *N* with other TW IBVs and US IBVs (Fig. 6). During the 1970s in Taiwan, flocks were extensively immunised with the Mass-serotype H120 vaccine (Lu et al., 1993). In this study, our finding suggests that the recombination in the *N* gene produced a novel IBV founder distinct from IBV lineages present before 1964. However, we did not exclude the possibility that the vaccination may also contribute to the antigenic shift of TW IBVs. The recombination event may have provided replication benefits, enabling the offspring of this founder to become dominant. To increase fitness under the pressure of H120 vaccination, the TW IBV with *N* recombinant might have undergone positive selection to escape from immune surveillance or to gain a replication advantage within quasi species.

Acknowledgments

This work was supported by the Bureau of Animal and Plant Health Inspection and Quarantine, Council of Agriculture in Taiwan (grant number 95AS-13.2.1-BQ-BE). It is highly appreciated. We also thank Dr. Yi-Ling Lin at the Institute of Biomedical Sciences in Academia Sinica

for critical reading of this manuscript and valuable comments.

Appendix A. Supplementary data

Supplementary data associated with this article can be found, in the online version, at [doi:10.1016/j.vetmic.2010.02.027](https://doi.org/10.1016/j.vetmic.2010.02.027).

References

- Cavanagh, D., 2007. Coronavirus avian infectious bronchitis virus. *Vet. Res.* 38, 281–297.
- Chen, H.W., Huang, Y.P., Wang, C.H., 2009. Identification of Taiwan and China-like recombinant avian infectious bronchitis viruses in Taiwan. *Virus Res.* 140, 121–129.
- Dolz, R., Pujols, J., Ordonez, G., Porta, R., Majo, N., 2008. Molecular epidemiology and evolution of avian infectious bronchitis virus in Spain over a fourteen-year period. *Virology* 374, 50–59.
- Eigen, M., 1987. New concepts for dealing with the evolution of nucleic acids. *Cold Spring Harb. Symp. Quant. Biol.* 52, 307–320.
- Gelb, J.J., Jackwood, M.W., 1998. Infectious bronchitis. In: Swayne, D.E., Glisson, J.R., Jackwood, M.W., Pearson, J.E., Reed, W.M. (Eds.), *A Laboratory Manual for the Isolation and Identification of Avian Pathogens*. American Association of Avian Pathologists: Kennett Square, pp. 169–174.
- Holmes, E.C., Rambaut, A., 2004. Viral evolution and the emergence of SARS coronavirus. *Philos. Trans. R. Soc. Lond. Biol. Sci.* 359, 1059–1065.
- Hon, C.C., Lam, T.Y., Shi, Z.L., Drummond, A.J., Yip, C.W., Zeng, F., Lam, P.Y., Leung, F.C., 2008. Evidence of the recombinant origin of a bat severe acute respiratory syndrome (SARS)-like coronavirus and its implications on the direct ancestor of SARS coronavirus. *J. Virol.* 82, 1819–1826.
- Huang, Y.P., Lee, H.C., Cheng, M.C., Wang, C.H., 2004. S1 and N gene analysis of avian infectious bronchitis viruses in Taiwan. *Avian Dis.* 48, 581–589.
- Huang, Y.P., Wang, C.H., 2006. Development of attenuated vaccines from Taiwanese infectious bronchitis virus strains. *Vaccine* 24, 785–791.
- Jia, W., Karaca, K., Parrish, C.R., Naqi, S.A., 1995. A novel variant of avian infectious bronchitis virus resulting from recombination among three different strains. *Arch. Virol.* 140, 259–271.
- Keck, J.G., Soe, L.H., Makino, S., Stohlman, S.A., Lai, M.M., 1988. RNA recombination of murine coronaviruses: recombination between fusion-positive mouse hepatitis virus A59 and fusion-negative mouse hepatitis virus 2. *J. Virol.* 62, 1989–1998.
- Keck, J.G., Stohlman, S.A., Soe, L.H., Makino, S., Lai, M.M., 1987. Multiple recombination sites at the 5'-end of murine coronavirus RNA. *Virology* 156, 331–341.
- Kosakovsky Pond, S.L., Posada, D., Gravenor, M.B., Woelck, C.H., Frost, S.D., 2006. GARD: a genetic algorithm for recombination detection. *Bioinformatics* 22, 3096–3098.
- Kottier, S.A., Cavanagh, D., Britton, P., 1995. Experimental evidence of recombination in coronavirus infectious bronchitis virus. *Virology* 213, 569–580.
- Kusters, J.G., Jager, E.J., Niesters, H.G., van der Zeijst, B.A., 1990. Sequence evidence for RNA recombination in field isolates of avian coronavirus infectious bronchitis virus. *Vaccine* 8, 605–608.
- Lai, M.M., Baric, R.S., Makino, S., Keck, J.G., Egbert, J., Leibowitz, J.L., Stohlman, S.A., 1985. Recombination between nonsegmented RNA genomes of murine coronaviruses. *J. Virol.* 56, 449–456.
- Liao, C.L., Lai, M.M., 1992. RNA recombination in a coronavirus: recombination between viral genomic RNA and transfected RNA fragments. *J. Virol.* 66, 6117–6124.
- Lin, K.Y., Wang, H.C., Wang, C.H., 2005. Protective effect of vaccination in chicks with local infectious bronchitis viruses against field virus challenge. *J. Microbiol. Immunol. Infect.* 38, 25–30.
- Liu, S.W., Zhang, Q.X., Chen, J.D., Han, Z.X., Liu, X., Feng, L., Shao, Y.H., Rong, J.G., Kong, X.G., Tong, G.Z., 2006. Genetic diversity of avian infectious bronchitis coronavirus strains isolated in China between 1995 and 2004. *Arch. Virol.* 151, 1133–1148.
- Lu, Y.S., Shieh, H.K., Tsai, H.J., Lin, D.F., Lee, Y.L., 1993. The incidence and virus isolation of infectious bronchitis in chickens in Taiwan. *Chin. Soc. Vet. Sci.* 19, 119–129.
- Magiorkinis, G., Magiorkinis, E., Paraskevis, D., Vandamme, A.M., Van Ranst, M., Moulton, V., Hatzakis, A., 2004. Phylogenetic analysis of

- the full-length SARS-CoV sequences: evidence for phylogenetic discordance in three genomic regions. *J. Med. Virol.* 74, 369–372.
- Makino, S., Keck, J.G., Stohlman, S.A., Lai, M.M., 1986. High-frequency RNA recombination of murine coronaviruses. *J. Virol.* 57, 729–737.
- Martin, D., Rybicki, E., 2000. RDP: detection of recombination amongst aligned sequences. *Bioinformatics* 16, 562–563.
- Maynard Smith, J., Szathmáry, E., 1995. *The Major Transitions of Evolution*. Freeman, Oxford.
- Posada, D., Crandall, K.A., 1998. MODELTEST: testing the model of DNA substitution. *Bioinformatics* 14, 817–818.
- Rodriguez, F., Oliver, J.L., Marin, A., Medina, J.R., 1990. The general stochastic model of nucleotide substitution. *J. Theor. Biol.* 142, 485–501.
- Stavrínides, J., Guttman, D.S., 2004. Mosaic evolution of the severe acute respiratory syndrome coronavirus. *J. Virol.* 78, 76–82.
- Wang, C.H., Hsieh, M.C., Chang, P.C., 1996. Isolation, pathogenicity, and H120 protection efficacy of infectious bronchitis viruses isolated in Taiwan. *Avian Dis.* 40, 620–625.
- Wang, C.H., Huang, Y.C., 2000. Relationship between serotypes and genotypes based on the hypervariable region of the S1 gene of infectious bronchitis virus. *Arch. Virol.* 145, 291–300.
- Wang, C.H., Tsai, C.T., 1996. Genetic grouping for the isolates of avian infectious bronchitis virus in Taiwan. *Arch. Virol.* 141, 1677–1688.
- Wang, L., Junker, D., Collisson, E.W., 1993. Evidence of natural recombination within the S1 gene of infectious bronchitis virus. *Virology* 192, 710–716.
- Wang, X., Khan, M.I., 2000. Molecular characterization of an infectious bronchitis virus strain isolated from an outbreak in vaccinated layers. *Avian Dis.* 44, 1000–1006.
- Yu, L., Jiang, Y., Low, S., Wang, Z., Nam, S.J., Liu, W., Kwangac, J., 2001. Characterization of three infectious bronchitis virus isolates from China associated with proventriculus in vaccinated chickens. *Avian Dis.* 45, 416–424.
- Zhang, X.W., Yap, Y.L., Danchin, A., 2005. Testing the hypothesis of a recombinant origin of the SARS-associated coronavirus. *Arch. Virol.* 150, 1–20.